Vol. 729: 219–232, 2024
https://doi.org/10.3354/meps14510

MARINE ECOLOGY PROGRESS SERIES
Mar Ecol Prog Ser

Published February 22

Humpback–krill relationships are strongest at fine spatial scales in the Northern California Current region

Rachel L. Kaplan[1,2,*], Solène Derville[2], Kim S. Bernard[1], Elizabeth M. Phillips[3], Leigh G. Torres[2]

[1]College of Earth, Ocean, and Atmospheric Sciences, Oregon State University, Corvallis, Oregon 97331, USA
[2]Geospatial Ecology of Marine Megafauna Lab, Marine Mammal Institute, Department of Fisheries, Wildlife and Conservation Sciences, Oregon State University, Newport, Oregon 97365, USA
[3]Fishery Resource Analysis and Monitoring Division, Northwest Fisheries Science Center, National Marine Fisheries Service, National Oceanic and Atmospheric Administration, Seattle, Washington 98112, USA

ABSTRACT: Understanding scale-dependent variability in predator–prey relationships is essential to ecosystem management. The Northern California Current (NCC) ecosystem is an important foraging ground for humpback (*Megaptera novaengliae*) and other rorqual whales, but it is also an area that presents diverse anthropogenic threats. Clarifying the most meaningful spatial scale to analyze relationships between whales and krill, a key prey item, is important to understanding ecosystem function and informing research and management efforts. To examine spatially explicit relationships between humpback whales and krill in the NCC, we analyzed concurrent whale sightings and acoustically detected krill abundance estimates collected in May and September between 2018 and 2022. We used generalized additive mixed models to predict humpback whale occurrence at a series of ecologically relevant nested spatial scales: 1, 2, 5, and 20 km. We found that relative krill abundance at a spatial scale of 5 km had the greatest influence on humpback whale occurrence. Our results suggest that whale and krill relationships at the 5 km scale may be both energetically profitable for whales to optimize foraging efficiency and also most detectable using our traditional methodological approaches (paired observer and echosounder surveys). We recommend that zooplankton prey data at the 5 km scale be incorporated into future humpback whale distribution models and considered for management applications in this region.

KEY WORDS: Active acoustics · Humpback whales · Spatial ecology · Prey · Foraging habitat · Krill · Northern California Current

1. INTRODUCTION

Trophic relationships drive the function of communities, flow of energy through ecosystems, and biogeochemical cycles integral to the earth system (Lindeman 1942). Predator–prey relationships both result from and control the distribution of species, causing feedback loops on species' behavior, genetics, and evolution (Barbosa & Castellanos 2005). Across diverse environments, ecological studies have revealed how distributions of prey structure those of predators, from the inverse and cyclical population dynamics of lynx and snowshoe hare across Canada (Elton & Nicholson 1942), to multiscale distributions of murres and capelin in the Barents Sea (Fauchald et al. 2000), to penguins foraging for fish in shallow eastern Australian waters (Carroll et al. 2017).

Prey in many ecosystems exist within a hierarchical framework of patches that contain nested spatiotemporal scales (Kotliar & Wiens 1990). Ecological rela-

*Corresponding author: kaplarac@oregonstate.edu

Publisher: Inter-Research · www.int-res.com

tionships between predators and prey differ depending on the scale of observation; thus, identifying the most relevant scales at which to observe, understand, and manage these relationships is complex. Ecosystems are characterized by variability across a range of spatial and temporal scales, and the act of observation intrinsically biases the relationships perceived (Levin 1992). The issue of scale is particularly pertinent in marine environments, which are highly dynamic and characterized by resource patchiness. This inherent complexity is evident in the divergent results of studies that seek to link predator and prey distributions in the marine environment. For example, incorporating prey data into fine-scale species distribution models did not improve predictions of bottlenose dolphin *Tursiops truncatus* occurrence in Florida Bay in the southeastern USA (Torres et al. 2008). By contrast, metrics of krill *Nyctiphanes australis* abundance improved predictions of the fine-scale distribution of blue whales *Balaenoptera musculus brevicauda* in New Zealand's South Taranaki Bight (Barlow et al. 2020), and acoustic data describing the Western Antarctic Peninsula preyscape improved predictions of relative humpback *Megaptera novaeangliae* and minke *B. acutorstrata* whale abundance at fine spatial scales (Friedlaender et al. 2006). Thus, the spatial scale at which prey is sampled relative to predators influences ecological conclusions, and proxy environmental data may yield more informative predictions when prey data at an appropriate scale are unavailable (Torres et al. 2008). Other studies have used satellite tracking and multiple descriptors of prey quantity to document positive relationships between fine-scale prey patches and individual whales, seals, and seabirds (e.g. Benoit-Bird et al. 2013, Ryan et al. 2022).

Appreciating scale-dependent variability in ecological relationships is essential to developing a sound understanding of ecosystems, and to managing them (Levin 1992). Such efforts may be particularly crucial based on the life history traits of the animals concerned. Humpback whales are capital breeders, relying on stored energy reserves to complete their migrations between foraging and breeding grounds, and to reproduce (Dawbin 1966). Exploiting prey resources efficiently during the limited time spent on foraging grounds is key for humpback migration timing, survivorship, and reproductive success. Every spring, several populations of humpback whales (Central American, Mexican, and Hawaiian distinct population segments; NOAA 2016) migrate from low-latitude calving grounds to important foraging grounds in the Northern California Current (NCC) region off the US west coast. One of the globe's 4 eastern boundary current systems, the California Current extends from the transition zone separating the North Pacific and Alaska gyres in the northern Pacific Ocean to Baja California, Mexico, in the south (Checkley & Barth 2009). Wind-driven upwelling drives seasonal nutrient input and high biological productivity both along the continental shelf and offshore, supporting krill and other zooplankton as well as predatory fish, seabirds, cetaceans, and pinnipeds (Checkley & Barth 2009). Two species of krill, *Euphausia pacifica* and *Thysanoessa spinifera*, are abundant in this region and are targeted by foraging rorqual whales, including humpback whales (Brinton 1962).

Krill are patchily distributed and undergo diel vertical migration, taking refuge from predators at depth during the day and moving to the surface to feed at night (Brinton 1967). Humpback whales are capable of prey-switching in response to changes in prey composition and availability driven by oceanographic and environmental conditions. Humpback whales target krill during positive phases of the North Pacific Decadal Oscillation (PDO) and switch to foraging on schooling fish during negative phases of the PDO (Fleming et al. 2016). This ability to prey-switch can create complex predator–prey dynamics and increase the risk of whale–fishery interactions. For example, anomalously low krill abundance in the central California Current region during a 2014–2015 marine heatwave led humpback whales to target inshore anchovy schools, resulting in an increase in fisheries entanglement events (Santora et al. 2020). Humpback whales also change the depth at which they forage based on vertical prey availability. In particular, they may target shallower prey when available to reduce the additional energetic costs of feeding at depth, which requires longer dives and extended breath holding (Goldbogen et al. 2012, Friedlaender et al. 2013, Tyson et al. 2016, Nichols et al. 2022).

Recent work has examined humpback–prey relationships at multiple scales in the broader California Current large marine ecosystem (CCLME), with the aim to enhance understanding of ecosystem function and inform ecosystem-based management (e.g. Fleming et al. 2016, Rockwood et al. 2020, Santora et al. 2020). A multiscale study utilized telescoping spatial scales (25, 50, and 100 km) and incorporated multiple prey types (herring, anchovy, krill) to describe relationships between humpback whales and prey across the CCLME (Szesciorka et al. 2023). While whale abundance was not strongly correlated with prey biomass, models based on the number of proximate prey

hotspots had stronger predictive capacity (Szesciorka et al. 2023). Clarifying the most meaningful spatial scale at which to analyze humpback–prey relationships in this region is important to understanding ecosystem function, anticipating humpback whale response to climate change, and informing research and management.

Whales throughout the CCLME are threatened by diverse anthropogenic impacts, including entanglement, ship strikes, noise, water quality, and marine debris (Oldach et al. 2022). Hence, there is a direct management need to understand the impactful scales of relationships between whales and prey in the NCC region (Derville et al. 2023). Krill is abundant relative to other prey types in the NCC region (Szesciorka et al. 2023), and *E. pacifica* and *T. spinifera* (hereafter 'krill') are considered the main component of the preyscape for humpback whales. In this study, we explore humpback–krill relationships and clarify the meaningful spatial scales at which these relationships operate in the NCC region. We use a data set of concurrent daytime humpback whale visual observations and acoustically derived krill abundance estimates collected during May and September over 4 years (2018–2022) to model relationships across multiple spatial scales, with the objective of identifying the most relevant scale of prey driving humpback whale distributions. We also conducted a parallel analysis using additional fin whale and unidentified rorqual whale observations to learn about the stability of these predator–prey relationships for all rorqual species in the NCC (see the Appendix). By using data from standardized surveys that are repeated both intra- and interannually, we can quantify these predator–prey relationships in the NCC region at broader spatiotemporal scales than previous studies and characterize variability to enable predictions of future change. Using data collected through a time series of long-term standardized repeated surveys offers the opportunity to identify trends in predator–prey interactions that short-term studies cannot provide.

As humpback whales visit our study area to feed, we expected predator–prey overlap to become more congruent as spatial scales reduce. Therefore, we hypothesized that associations between whales and krill during the day are strongest at the finest spatial scales and decline at increasing scales (1 > 2 > 5 > 20 km). As no common definition of scale resolution from fine to coarse exists across the fields of oceanography and spatial ecology (e.g. Stommel 1963, Mannocci et al. 2017, Torres 2017), we refer to 1 and 2 km as very fine scale, 5 km as fine scale, and 20 km as mesoscale.

2. MATERIALS AND METHODS

2.1. Whale data collection and processing

From 2018 to 2022, marine mammal observers collected cetacean distribution data during research cruises aboard the NOAA Ship 'Bell M. Shimada'. These cruises were conducted in May and September, and they transited between La Push, WA, to Crescent City, Trinidad, or San Francisco, CA, USA, sampling oceanographic stations up to 200 nautical miles (nmi) offshore (Fig. 1). Observers collected data during transits between oceanographic stations, following a distance sampling protocol (Buckland et al. 2015). A handheld GPS was used to record the trackline of the ship, which was subsequently interpolated to 1 position every 30 s to ensure consistency across surveys. Survey speed averaged 10 knots, with occasional periods of 5 knot travel due to other research needs. Observers (typically 2) were positioned on either side of the vessel's flying bridge, 13 m above the waterline; during poor survey conditions, they would transition to the bridge, 10.5 m above the waterline. During on-effort survey periods, observers constantly scanned from the ship to the horizon for animals, using binoculars at least 30% of the time. Individual whales were identified to species if a positive visual ID was possible and were recorded as unidentified if not. Group sizes were estimated conservatively based on the number of simultaneous observations of whales within a sighting. In addition, the angle of the animal to the trackline at the point of first observation was estimated and recorded. Radial distance was estimated visually for animals within 1 km and by using binocular reticles for those farther away (Fujinon 7 × 50s). These data were used to trigonometrically derive geographic coordinates of the sighted whales using the 'geosphere' R package (version 1.5-14). Whale groups that included either humpback whales or unidentified rorqual whales were considered for further analysis (see Table 1, Fig. 1).

2.2. Acoustic data collection and processing

Acoustic data were collected via hull-mounted, downward-looking Simrad EK60 (in 2018) and EK80 (in 2019–2022) narrow-band split-beam echosounders operating at multiple frequencies (18, 38, 70, 120, and 200 kHz). Data were recorded continuously from the surface to a depth of 750 or 1000 m using a 1.024 ms narrow-band pulse at rates ranging between 1 ping s^{-1} to 1 ping per 8 s, depending on bottom depth.

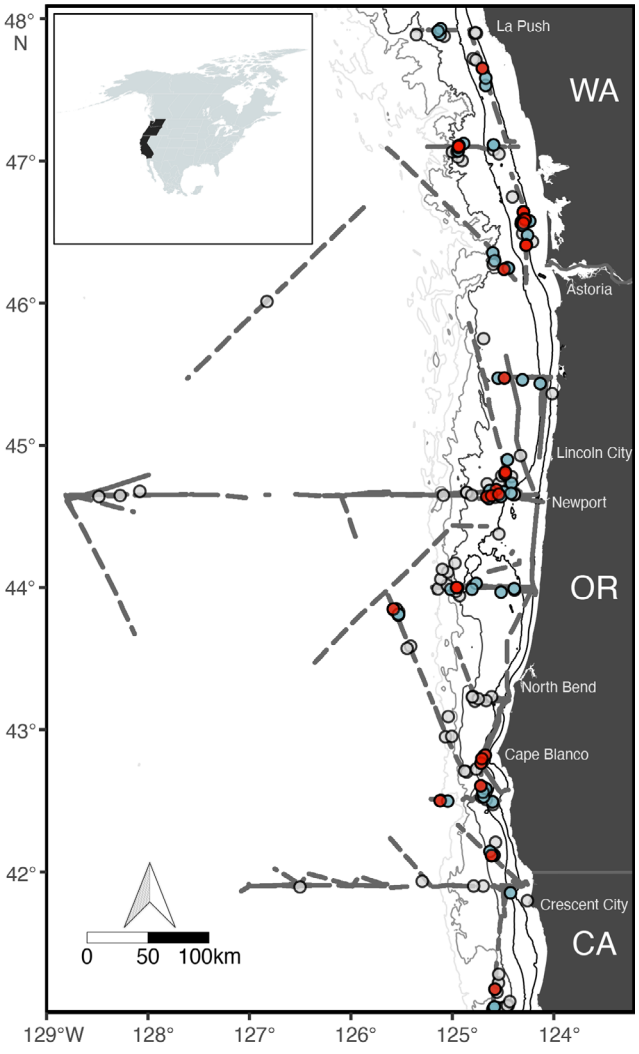

Fig. 1. Concurrent echosounder data and whale surveys (gray lines) in the Northern California Current region off northern California, Oregon, and Washington (US West Coast). Red dots: humpback whale groups included in Models 1–4; light blue dots: additional humpback whale groups included in the final model (Model 5); gray dots: other rorqual whale observations (see Appendix for results of rorqual–krill models). Isobaths (50, 100, 500, 1000, and 1500 m) are represented by gray lines (deeper isobaths are shown in progressively lighter colors)

Acoustic data were processed using Echoview (version 13.1; Echoview) following the workflow described in Phillips et al. (2022). Background noise was estimated based on the mean volume backscattering strength (MVBS or S_v; dB re 1 m^{-1}) in 40 ping × 10 m cells and was removed by subtracting estimated background noise from the original signal using a maximum noise threshold of −125 dB and a 10 dB signal-to-noise ratio threshold (De Robertis & Higginbottom 2007). Impulse noise spikes were removed using a dedicated Echoview operator. The bottom was detected acoustically and corrected manually as needed to omit seafloor echoes and bottom intrusion, which was minimized by a 2 m offset. In addition, data within 30 m of the water surface were omitted to remove surface noise and bubbles and to account for the near-field range of the 38 kHz echosounder. Though this exclusion may omit krill backscatter near the sea surface and seafloor, our study focused on daytime distributions of adult krill, which have been shown to primarily occur between approximately 100 and 250 m (Mackas et al. 1997, Phillips et al. 2022). Data from below a depth of 300 m were excluded to account for a decreased signal-to-noise ratio with depth, especially for the 120 kHz frequency. Acoustic data were also omitted when vessel speeds dropped below 5 knots. Data are reported as nautical area scattering coefficient (NASC; m^2 nmi^{-2}), which is a relative index of abundance and a proxy for biomass. Because the data were collected using uncalibrated echosounders, we did not attempt to compare overall abundance of krill between years but instead focused on relationships between relative krill abundance and whales within each survey.

2.3. Krill identification and quantification

We used frequency differencing to classify krill in the acoustic data, based on published ranges for krill in the North Pacific (De Robertis et al. 2010) and previous efforts in the region (Phillips et al. 2022). We first aligned our data in Echoview by matching 120 kHz cells to 38 kHz cells in space and time using ping times and sample geometry, and we used a $\Delta MVBS_{120\text{-}38}$ range of 10.0–16.3 dB to classify krill from other backscatter. We then used an integration threshold of −70 dB to export georeferenced volumetric S_v and NASC at 120 kHz, integrated in 10 × 10 m bins.

These data were scrutinized for possible contamination by noise spikes or inclusion of targets like small fish with swim bladders by visually examining cells with mean S_v values between −35 and −45 dB and removing noise manually if needed. Cells with an S_v value of −80 dB or below were then set to 0 to omit weak signals that represented less than 3–4 krill m^{-3} (Phillips et al. 2022). Due to zero inflation, we logged the krill NASC data for further analyses.

2.4. Whale–krill analysis

To examine *in situ* relationships, georeferenced whale and krill data were matched in space and time.

Krill data were restricted to daytime (1 h after sunrise to sunset) on-effort periods of concurrent whale observations. Due to sample size limitations, only humpback whale observations associated with concurrent krill data were included in our hierarchical scale analysis. All analyses were conducted in R 4.2.3 (R Core Team 2023). The data were projected in the Universal Transverse Mercator system, and concentric circles (hereafter referred to as buffers) with radii of 1, 2, 5, and 20 km were drawn around all rorqual whale observations (Fig. 2; 'sf' R package, version 1.0-8). Given that only humpback whales were included in this analysis, krill data in the vicinity of other rorqual whales (e.g. blue, fin, or unidentified whales) that also target krill patches were removed in order to ensure the preyscape surrounding our species of interest (humpback whales) was compared to control conditions when no whales were present. Krill data were assigned as being within or outside the area of each buffer, and we plotted the vertical distribution of relative krill abundance within each of the 4 buffer sizes. Based on these vertical distribution plots, NASC was averaged within 30–50, 50–100, 100–200, and 200–300 m depth bins calculated within each buffer for further comparisons to humpback whale observations. We checked for cross-correlation between depth bins and found a maximum Pearson's pairwise correlation of 0.36, indicating that we could retain all 4 depth bins for modeling purposes ('corrplot' R package, version 0.92). Because whales were located at varying distances from the trackline, the amount of underway acoustic data included within each buffer varied across sightings but always exceeded 100 m of on-effort horizontal trackline (e.g. at the 1 km scale, between 18 and 215 bins of 10 m NASC data points were included).

To compare and quantify the relationships between krill and humpback whales at 4 spatial scales, we generated generalized additive mixed models (GAMMs, 'mgcv' R package version 1.8-42; Wood 2011) quantifying the probability of humpback whale occurrence (a presence–absence binomial response) in relation to krill relative abundance measured at 1, 2, 5, and 20 km. GAMMs use data-defined smoothing ele-

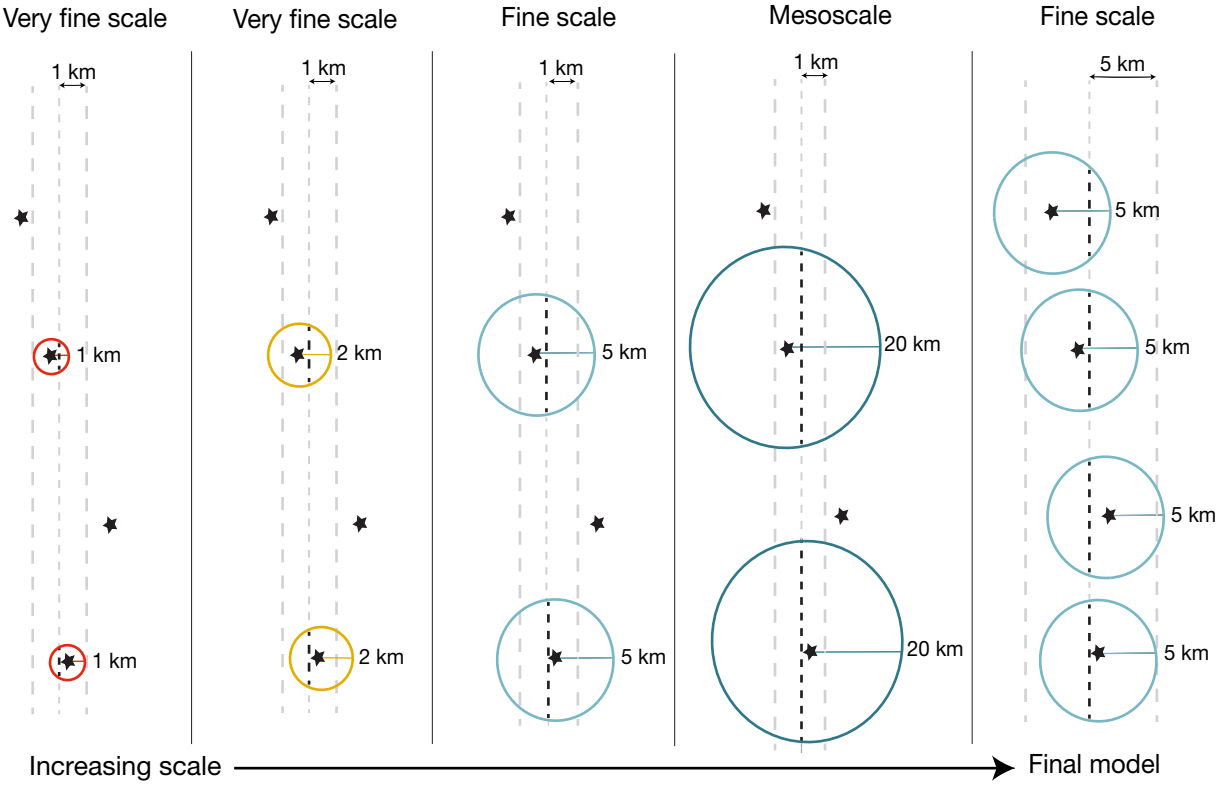

Fig. 2. Schematic representation of the inputs to the hierarchical scale and final models. The distance thresholds for included observations (coarse dashed lines) are illustrated around the ship's trackline (fine dashed line). Echosounder data along the trackline may be inside the buffers (black) or outside (gray), depending on model spatial scale. Buffer radii drawn at increasing spatial scales (circles color-coded from 1 to 20 km) are drawn around humpback whale observations (black stars). The leftmost panel represents the data included in the 1 km 'very fine scale' model; model spatial scale increases moving right. The rightmost panel represents the inputs for the final, fine scale model. This schematic is not drawn to scale

ments to model non-linear responses to a set of predictors (Elith & Leathwick 2009). We selected GAMMs for their capacity to adeptly represent realistic ecological relationships and accommodate complex interactions between species distributions and environmental variability (Torres et al. 2008), which makes them useful for modeling marine mammal distributions (Derville et al. 2018, Orphanides et al. 2023, Szesciorka et al. 2023). Cruise ID was included as a random effect in the models to account for variability in effort and environmental conditions between surveys. The influence of krill vertical distribution was included using an interaction term between krill NASC and depth bin. Whale group size was accounted for through weights equal to the number of individuals comprising a whale group within a given spatial scale so that fitted trends would be more strongly driven by large groups of foraging whales than by singletons. GAMMs were fitted with a binomial response distribution using a logit link function and a restricted maximum likelihood method ('bam' and 'fREML', 'mgcv' R package, version 1.8-42). The effect of krill relative abundance on humpback whale occurrence was modeled with penalized thin-plate regression splines with basis size limited to 5 to prevent overfitting (Wood 2017). Variable selection was conducted with a shrinkage approach implemented in the 'mgcv' R package, which adds an extra penalty to each smoother and penalizes non-significant variables to zero (Marra & Wood 2011). Model fit was evaluated based on the percent deviance explained, as calculated and reported by 'mgcv' for a binomial error distribution (Wood 2011).

Our 4 hierarchical scale models were generated with krill data collected across all whale survey transects, and designated as falling within or outside buffers (1, 2, 5, 20 km) drawn around a subset of humpback whale groups observed within 1 km of the trackline (n = 29 humpback whale groups; see Table 2). This set of hierarchical scale models consists of Model 1 (1 km scale), Model 2 (2 km scale), Model 3 (5 km scale), and Model 4 (20 km scale). We generated a final model using 5 km buffers drawn around a subset of humpback whale groups found within 5 km of the trackline (n = 79 humpback whale groups) and krill data collected along the transect that fell within or outside these 5 km buffers (see Fig. 2 for a schematic representation). In addition, we also replicated this same approach in a supplementary analysis using all rorqual whale observations, which included fin whales, humpback whales, and unidentified rorqual whales (n = 235 individuals in 178 groups; Table A1, Figs. A1 & A2 in the Appendix; Models A1–A4) and their associated acoustic data in order to characterize these relationships more broadly for baleen whales in the NCC.

3. RESULTS

A total of 670 rorqual whales (1–10 individuals per group) were sighted during 19 288 km of survey effort during 8 cruises between 2018 and 2022 (Table 1). Krill were detected throughout our study area during each survey (mean log-NASC over n = 580 710 bins: 2.45 m^2 nmi^{-2}; 10.55 m^2 nmi^{-2} unlogged), and the relative abundance of krill in the vicinity of whales increased with the spatial scale of observation (i.e. with buffer size; 1-way ANOVA, F = 3.8, df = 3, p = 0.011; Fig. 3). Relative to concurrently observed whales, less krill (log NASC m^2 nmi^{-2}) was detected at a 1 km very fine scale (mean ± SD: 13.83 ± 0.66), compared to the 20 km mesoscale (28.80 ± 0.86; post hoc Tukey test, adjusted p-value [p_{adj}] = 0.018), and there was no significant difference between krill relative abundance detected at the 20 km mesoscale and the 5 km fine scale (post hoc Tukey test, p_{adj} = 0.541).

The subset of humpback whale observations (n = 29 groups of 37 individuals) made within 1 km of the ship's trackline was used in Model 1 (1 km scale), Model 2 (2 km scale), Model 3 (5 km scale), and Model 4 (20 km scale). Model deviance explained increased with buffer size from 14.1% at 1 km, to

Table 1. Concurrent active acoustics and whale observation data collection (km and days) per cruise, and all rorqual whale and humpback whale groups observed and included in models

Year	Month	Effort (km)	Effort (days)	Humpback whale groups used in this study (Models 1–4 / 5)	All rorqual whale groups / average group size used in rorqual-krill models (see the Appendix)
2018	May	3516.9	9	6 / 10	21 / 1.9
	September	2561.2	9	1 / 3	9 / 1.1
2019	May	3015.0	10	0	0
	September	1952.5	9	3 / 9	22 / 2.4
2020	September	3030.3	11	8 / 34	73 / 1.2
2021	May	257.6	10	0	5 / 1.7
2022	May	3562.1	12	18 / 47	102 / 1.2
	September	1392.4	5	1 / 2	3 / 1

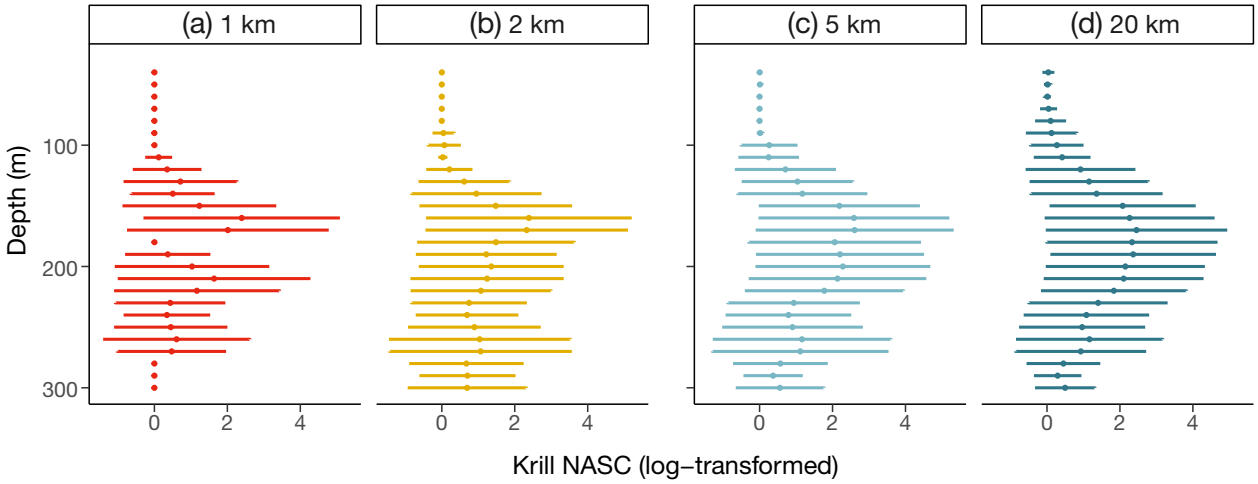

Fig. 3. Average depth distribution of krill relative abundance (nautical area scattering coefficient [NASC], m^2 nmi^{-2}) at each buffer radius scale surrounding the sighted humpback whales. Standard deviations are shown as horizontal bars across each point. Note that mean NASC values below 1 appear as zeroes on the log-transformed *x*-axis

18.7% at 2 km, to 25.2% at 5 km, to a maximum of 36.0% at the 20 km scale (Table 2). However, marginal deviance explained, which describes the contribution of krill NASC to the explanatory power of the model, increased with scale to a maximum at the 5 km scale (3.8%; Model 3) and then declined at the 20 km mesoscale (2.5%; Model 4). We use the amplitude of the fitted response on the *y*-axis as an indicator of variable influence, which shows that overall, krill positively influenced whale occurrence at all spatial scales and depth bins, and relationships were generally stronger at smaller scales and shallower depth bins (Fig. 4). In the shallowest layer (30–50 m), the relationship peaks for all scales at high log-transformed NASC values (>5 m^2 nmi^{-2}; Fig. 4). In the 100–200 m bin, the response curves at all scales first peak at a log-transformed NASC value of 2 m^2 nmi^{-2} and either remain generally uniform after (1 and 20 km) or continue to increase (2 and 5 km). In the 50–100 and 200–300 m depth bins, the influence of krill on whale presence was strongest at 5 and 20 km. Across all depth layers and all spatial scales, the response curves illustrating the effect of krill on whale presence crossed the zero line to become positive

Table 2. Summary of humpback whale–krill association models at each spatial scale (buffer radius). For each model, we report conditional and marginal deviance explained, the number of humpback whale groups included (N_{wh}), and the absence, presence, and total number of data points in each model (N). For each smooth term (e.g. NASC 30–50 m, NASC 50–100 m, etc.) and the random effect (survey), we report estimated degrees of freedom (edf) and *F*-statistics. NASC (Nautical Area Scattering Coefficient, m^2 nmi^{-2}) is a relative abundance metric for krill. All approximate significance of smooth terms showed $p < 0.0001$

Scale	Model	Buffer radius (km)	N_{wh}	N (absence, presence)	Conditional deviance explained (%)	Marginal deviance explained (%)	NASC 30–50 m	NASC 50–100 m	NASC 100–200 m	NASC 200–300 m	Survey
Very fine	1	1	29	604849 (594477, 10372)	14.1	1.34	edf = 2.264, *F* = 236	edf = 1.002, *F* = 265	edf = 3.918, *F* = 782	edf = 2.652, *F* = 330	edf = 6.711, *F* = 1573
Very fine	2	2	29	593845 (569424, 24421)	18.7	2.22	edf = 2.787, *F* = 2625	edf = 1.230, *F* = 2767	edf = 3.955, *F* = 4225	edf = 3.686, *F* = 1649	edf = 6.743, *F* = 3501
Fine	3	5	29	565945 (508332, 57613)	25.2	3.82	edf = 2.894, *F* = 3077	edf = 2.948, *F* = 3007	edf = 3.891, *F* = 8926	edf = 3.708, *F* = 6964	edf = 6.769, *F* = 7541
Meso	4	20	29	580710 (386409, 194301)	36.0	2.50	edf = 2.961, *F* = 2399	edf = 2.980, *F* = 2350	edf = 2.995, *F* = 3606	edf = 2.983, *F* = 20990	edf = 6.790, *F* = 20986
Fine (final model)	5	5	79	649376 (508332, 141044)	26.7	3.36	edf = 3.908, *F* = 2838	edf = 3.577, *F* = 2761	edf = 3.882, *F* = 9401	edf = 3.680, *F* = 9063	edf = 6.787, *F* = 14624

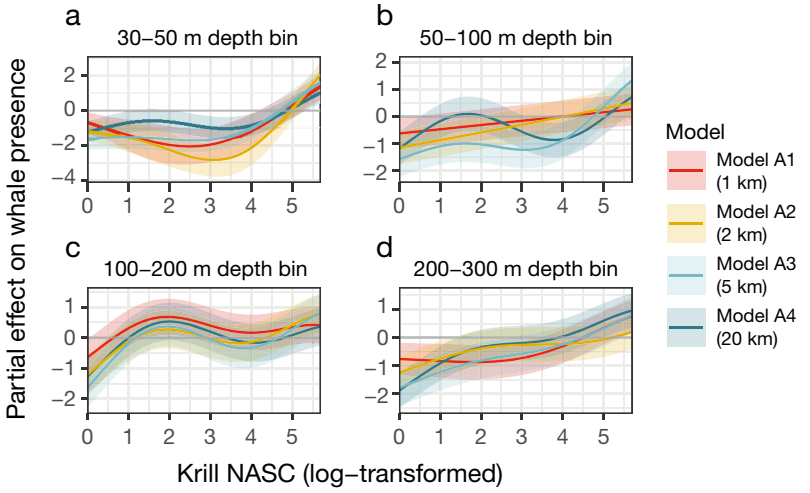

Fig. 4. Humpback whale–krill relationships modeled across multiple depth bins and spatial scales. Response curves represent the effect of the smooth function upon the trend in humpback whale presence, with higher values indicating higher predicted probability of occurrence. Shaded ribbons: 95% confidence intervals, colored per fitted trend. Log-transformed nautical area scattering coefficient (NASC; m^2 nmi^{-2}; a relative abundance metric for krill) is shown on the *x*-axis, limited to the 5^{th}–95^{th} percentiles of its distribution. All variables have significant p-values ($p < 0.0001$)

around a mean log-transformed NASC value of 4 m^2 nmi^{-2} (54.60 m^2 nmi^{-2} unlogged; note the confidence intervals indicating variability around the mean).

Given that relationships between whales and krill were strongest at the 5 km scale based on model marginal deviance explained (Table 2), an additional model was run at this scale using all humpback whale observations that had associated krill data within 5 km of the trackline (Model 5, n = 79 whale groups containing 105 individuals). We found that Model 5 had 26.7% conditional deviance explained and 3.4% marginal deviance explained, showing relatively similar performance to Model 3. In the 100–200 and 200–300 m depth bins, partial response to krill NASC was similar to Model 3, while the response was stronger in the 30–50 m depth bin and weaker in the 50–100 m depth bin than in Model 3 (Fig. 5). In models run across a larger set of all rorqual whales (see the Appendix), deviance explained increased from 15.6% at 1 km to 33.9% at 20 km, with a maximum marginal deviance explained of 2.6% at 5 km.

4. DISCUSSION

Our study illuminates the scale-dependent relationships that exist between humpback whales and krill, one of their key prey items. We found that krill relative abundance at a spatial scale of 5 km has the greatest correlation with humpback whale occurrence in the NCC region. This result speaks to both meaningful scales of observation and ecological relationships between humpback whales and their euphausiid prey, and it supports results from other modeling efforts in this region (Derville et al. 2022). A spatial scale of 5 km is likely optimal for analyzing the dynamic relationships between humpback whales and krill, and it can be used to develop and apply spatial management regulations, such as state efforts to mitigate entanglement risk to humpback and other protected whale species (e.g. ODFW 2021, 2022).

Contrary to our hypothesis, the models at very fine scales (1 and 2 km) did not perform as well as those at fine and meso scales (5 and 20 km). This result may indicate that acoustic prey data at very fine scales do not fully contextualize the foraging environment of a humpback whale. While the 20 km scale model (Model 4) had higher explanatory capacity than the 5 km scale model (Model 3), the influence of krill on whale presence was weaker, indicating that the 20 km scale may describe a prey environment that is less relevant or immediately perceptible to foraging whales. Mean krill NASC was not significantly greater at the 20 km scale than the 5 km scale, and the patchiness of the marine environment and tendency of krill to form discrete swarms (Brinton 1962) makes it likely

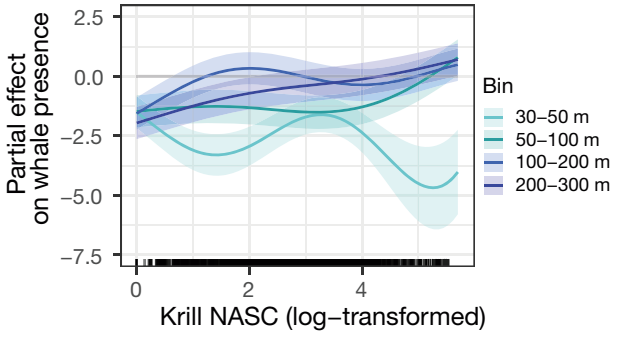

Fig. 5. Humpback whale–krill relationships modeled across depth bins at the 5 km scale in Model 5. Response curves represent the effect of the smooth function upon the trend in humpback whale presence, with higher values indicating higher predicted probability of occurrence. Shaded ribbons: 95% confidence intervals, colored per fitted trend. All variables have significant p-values ($p < 0.0001$). The rug plot along the *x*-axis represents all data points within the 5^{th}–95^{th} percentiles of the krill nautical area scattering coefficient (NASC) distribution (m^2 nmi^{-2}) across all depth bins

that areas of high NASC within a 20 km area are separated by more waters with minimal krill. Although a foraging whale may detect distant prey through chemoreception and audition (Torres 2017), faraway prey patches may not be as readily perceivable to a whale or they may simply not be worth the energy expenditure of increased travel and searching — particularly if the near environment remains favorable. From an observational standpoint, the 5 km scale may be coarse enough to average out fine-scale variation in prey density and describe the prey environment the whale can 'observe' (Levin 1992), while also being narrow enough that it is perceptible to a whale sensing the environment to locate patchy food resources (Torres 2017). We hypothesize that a 5 km area containing numerous and profitable prey patches offers whales an opportunity to minimize interpatch travel time and spend more time foraging to maximize energetic gain.

Ecologically speaking, these scale-dependent relationships between humpbacks and krill contextualize the landscape of choice that a humpback whale must navigate on the feeding grounds. Prey density must reach a certain threshold to elicit whale foraging effort and aggregation, activities which become unprofitable below this threshold (Piatt & Methven 1992). Optimal foraging theory predicts that an animal will choose to either maximize gained energy or minimize the time spent pursuing a given amount of energy (MacArthur & Pianka 1966). This 'time saving' approach is assumed to be adopted in favor of risk mitigation or the pursuit of other behaviors like reproduction (MacArthur & Pianka 1966). As humpback whales in our study area are on their foraging grounds, we assume individuals are attempting to maximize their gained energy by targeting the most advantageous krill patches. In our models, the steep functional response at intermediate krill relative abundances observed across spatial scales (i.e. near a log-transformed NASC value of 4 m^2 nmi^{-2}) may represent a threshold of profitability for foraging humpbacks. At some point during foraging, any individual prey patch will drop below the threshold of profitability, whether from exploitation or predator-avoidance behaviors by the prey, and the predator will move on to find a new patch (Charnov 1976). Marginal value theorem predicts that a predator acting to maximize its energetic gain will depart a prey patch when the marginal capture rate in the patch drops to the average for the broader environment (Charnov 1976). For baleen whales, which must balance the demands of prey capture and breath holding in a given foraging bout, even a prey patch above the environmental average may be insufficient (Hazen et al. 2015), and the additional costs of searching for and digesting prey necessitate efficient prey capture during the limited time humpback whales spend on the foraging grounds (Videsen et al. 2023). Areas that are profitable at the 5 km scale may offer the right balance between effort and reward, sustaining a whale above the threshold of foraging profitability.

In addition, the depth of krill patches may drive foraging habitat selection. At very fine spatial scales, the 30–50 m depth bin stands out as a strong predictor of whale presence (Fig. 4). Because this depth bin represents acoustic backscatter from a smaller area than the others due to the narrower vertical bin (20 m vs. 50 or 100 m) and exclusion of data shallower than 30 m, this result may be a conservative representation of the influence of shallow krill patches. Foraging humpback whales in the Western Antarctic Peninsula preferentially target shallow prey (Nichols et al. 2022), and feeding on near-surface krill *Euphausia superba* may allow a whale to maximize its energetic gain (Friedlaender et al. 2016, Tyson et al. 2016). Throughout the period of this study, the depth of maximum krill abundance was centered around 170 m (Fig. 3), which aligns with the findings from previous studies in the region (Brinton 1962, Phillips et al. 2022). Interestingly, whale presence as predicted by the 100–200 m depth bin exhibits a variable distribution across all models, likely reflecting the patchy distribution of krill at depth. Humpback whales can dive deeper than 400 m (Derville et al. 2020), but they may dive more shallowly during the night and based on season (Nichols et al. 2022). While krill undergo a diel vertical migration that takes them from deeper waters during the day to the sea surface at night, our study used daytime visual surveys that precluded us from assessing nighttime whale–krill relationships. Therefore, the daytime depth-based relationships we identified may differ from nighttime patterns.

Overall, these findings echo previous research illustrating the scale dependency of predator–prey spatiotemporal co-occurrence. Model outcomes depend upon the scales at which data are collected and analyzed (Wiens 1989), highlighting the role of methodology in ecological interpretation. A positive predictive relationship between blue whales and acoustically detected krill was found in New Zealand at a 4 km scale (Barlow et al. 2020), similar to our study. Findings from both studies contrast with Torres et al. (2008), who found that environmental predictors far outperformed prey metrics derived from net tows when modeling bottlenose dolphin distributions in Florida. Though these studies focused on different ecosystems and species, part of this discrepancy is

likely driven by the difference in methods for quantifying prey: discrete net tows versus continuous hydroacoustic surveys that are more spatially comprehensive and enable concurrent observation of the prey field in the vicinity of predators. Moreover, while several studies using tag data with high spatial and temporal resolution have shown strong relationships between prey and bulk-filter feeding predators (e.g. right whales, Baumgartner & Mate 2003; blue whales, Goldbogen et al. 2015), it is difficult to describe such fine-scale relationships based on visual survey data, which constitute a snapshot of predator distributions. The marginal deviance explained values characterizing our models are in line with other studies that use a visual detection approach (Lambert et al. 2019, Receveur et al. 2022, Szesciorka et al. 2023). Despite the lack of behavioral information within our data compared to that obtained by tracking studies (e.g. travel versus foraging states), our approach revealed relevant scales of predator–prey relationships.

Prey quality, as well as quantity, is crucial to energetic gain, and humpback whales may target larger and reproductive krill with higher energetic value, if available (Cade et al. 2022). For the purposes of this study, all krill were considered of equal quality, and we relied on NASC as a proxy for krill biomass as the sole prey metric. However, krill quality, aggregation structure, and biomass density have been shown to shape whale foraging behaviors and patch selection (Friedlaender et al. 2016, Miller et al. 2019, Cade et al. 2021). Differences between the nutritional value of krill species and developmental stages can have significant consequences for the foraging success and distributions of humpback whales, which may preferentially target the larger, more lipid-rich *Thysanoessa spinifera*, like other whale species (Fiedler et al. 1998). Krill nutritional quality, swarm structure, and the impact of changing ocean conditions on preferential foraging warrant further investigation. In addition to humpback whales, blue *Balaenoptera musculus* and fin *B. physalus* whales also forage on krill in the region (Fiedler et al. 1998). While our sample size of blue and fin whales was too small to perform the same hierarchical scale analysis, a model of all rorquals at the 5 km scale showed overall similar trends as seen for humpback whales, though differences in the shallower depth bins indicate interesting variability in these relationships, particularly at the 5 and 20 km spatial scales (see the Appendix). Future work should investigate whether these species show similar spatial relationships. Fin and blue whales are larger, and increased body size both facilitates and requires increased prey capture (Goldbogen et al. 2019). Thus, blue and fin whales foraging in the NCC may require larger-scale prey patches than humpbacks, and higher prey densities within them to meet their energetic needs.

These findings are salient to ecological relationships in the NCC ecosystem and to management efforts across the CCLME. Just as prey distributions are dynamic, so too are the responses of their predators and the needs of adaptive ecosystem management. Increased awareness of humpback–krill relationships can support tools and resources that benefit marine resource management (Rockwood et al. 2020, Santora et al. 2020). Incorporating fine-scale prey data may improve modeling efforts and predictions of how these animals and ecosystems will respond to ongoing and future ocean changes (Derville et al. 2022). As the 5 km model yielded the strongest relationship between humpback whales and krill relative abundance, we recommend that prey data at that scale be incorporated into future models and considered for management applications in the NCC, such as entanglement mitigation efforts and fisheries planning. Considering predator–prey relationships at methodologically and ecologically informed scales can allow us, as ecosystem observers, to find a compromise to the problem of scale, bridging the distance between what an animal experiences in the environment and what we can accurately describe and manage.

Acknowledgements. This research received financial support from the NOAA Species Recovery Grant (no. NA19NMF 4720109), the Oregon State University Marine Mammal Institute, the Oregon Department of Fish & Wildlife (ODFW), Oregon Sea Grant, and the National Science Foundation (NSF) Graduate Research Fellowship Program. We extend a tremendous thank you to NOAA Northwest Fisheries Science Center and the crew of the R/V 'Bell M. Shimada' (chief scientists A. Bolm, J. Fisher, and S. Zeman) for enabling and facilitating data collection, as well as the marine mammal observers R. Albertson, D. Barlow, C. Bird, A. Kownacki, and F. Sullivan.

LITERATURE CITED

Barbosa P, Castellanos I (2005) Ecology of predator–prey interactions. Oxford University Press, Oxford

Barlow DR, Bernard KS, Escobar-Flores P, Palacios DM, Torres LG (2020) Links in the trophic chain: modeling functional relationships between *in situ* oceanography, krill, and blue whale distribution under different oceanographic regimes. Mar Ecol Prog Ser 642:207–225

Baumgartner M, Mate B (2003) Summertime foraging ecology of North Atlantic right whales. Mar Ecol Prog Ser 264:123–135

Benoit-Bird KJ, Battaile BC, Heppell SA, Hoover B and others (2013) Prey patch patterns predict habitat use by

top marine predators with diverse foraging strategies. PLOS ONE 8:e53348
Brinton E (1962) The distribution of Pacific euphausiids. Bull Scripps Inst Oceanogr Univ Calif 8:21–270
Brinton E (1967) Vertical migration and avoidance capability of euphausiids in the California Current. Limnol Oceanogr 12:451–483
Buckland ST, Rexstad EA, Marques TA, Oedekoven CS (2015) Distance sampling: methods and applications. Springer International Publishing, Cham
Cade DE, Seakamela SM, Findlay KP, Fukunaga J and others (2021) Predator-scale spatial analysis of intra-patch prey distribution reveals the energetic drivers of rorqual whale super-group formation. Funct Ecol 35:894–908
Cade DE, Kahane-Rapport SR, Wallis B, Goldbogen JA, Friedlaender AS (2022) Evidence for size-selective predation by Antarctic humpback whales. Front Mar Sci 9: 747788
Carroll G, Cox M, Harcourt R, Pitcher BJ, Slip D, Jonsen I (2017) Hierarchical influences of prey distribution on patterns of prey capture by a marine predator. Funct Ecol 31:1750–1760
Charnov EL (1976) Optimal foraging: the marginal value theorem. Theor Popul Biol 9:129–136
Checkley DM, Barth JA (2009) Patterns and processes in the California Current System. Prog Oceanogr 83:49–64
Dawbin WH (1966) The Seasonal migratory cycle of humpback whales. In: Norris KS (ed) Whales, dolphins, and porpoises. University of California Press, Berkley, CA, p 145–170
De Robertis A, Higginbottom I (2007) A post-processing technique to estimate the signal-to-noise ratio and remove echosounder background noise. ICES J Mar Sci 64: 1282–1291
De Robertis A, McKelvey DR, Ressler PH (2010) Development and application of an empirical multifrequency method for backscatter classification. Can J Fish Aquat Sci 67:1459–1474
Derville S, Torres LG, Iovan C, Garrigue C (2018) Finding the right fit: comparative cetacean distribution models using multiple data sources and statistical approaches. Divers Distrib 24:1657–1673
Derville S, Torres LG, Zerbini AN, Oremus M, Garrigue C (2020) Horizontal and vertical movements of humpback whales inform the use of critical pelagic habitats in the western South Pacific. Sci Rep 10:4871
Derville S, Barlow DR, Hayslip C, Torres LG (2022) Seasonal, annual, and decadal distribution of three rorqual whale species relative to dynamic ocean conditions off Oregon, USA. Front Mar Sci 9:868566
Derville S, Buell TV, Corbett KC, Hayslip C, Torres LG (2023) Exposure of whales to entanglement risk in Dungeness crab fishing gear in Oregon, USA, reveals distinctive spatio-temporal and climatic patterns. Biol Conserv 281:109989
Elith J, Leathwick JR (2009) Species distribution models: ecological explanation and prediction across space and time. Annu Rev Ecol Evol Syst 40:677–697
Elton C, Nicholson M (1942) The ten-year cycle in numbers of the lynx in Canada. J Anim Ecol 11:215–244
Fauchald P, Erikstad KE, Skarsfjordi H (2000) Scale-dependent predator–prey interactions: the hierarchical spatial distribution of seabirds and prey. Ecology 81:773–783
Fiedler PC, Reilly SB, Hewitt RP, Demer D and others (1998) Blue whale habitat and prey in the California Channel Islands. Deep Sea Res II 45:1781–1801
Fleming AH, Clark CT, Calambokidis J, Barlow J (2016) Humpback whale diets respond to variance in ocean climate and ecosystem conditions in the California Current. Glob Change Biol 22:1214–1224
Friedlaender AS, Halpin PN, Qian SS, Lawson GL, Wiebe PH, Thiele D, Read AJ (2006) Whale distribution in relation to prey abundance and oceanographic processes in shelf waters of the Western Antarctic Peninsula. Mar Ecol Prog Ser 317:297–310
Friedlaender AS, Tyson RB, Stimpert AK, Read AJ, Nowacek DP (2013) Extreme diel variation in the feeding behavior of humpback whales along the western Antarctic Peninsula during autumn. Mar Ecol Prog Ser 494: 281–289
Friedlaender AS, Johnston DW, Tyson RB, Kaltenberg A and others (2016) Multiple-stage decisions in a marine central-place forager. R Soc Open Sci 3:160043
Goldbogen JA, Calambokidis J, Croll DA, McKenna MF and others (2012) Scaling of lunge-feeding performance in rorqual whales: mass-specific energy expenditure increases with body size and progressively limits diving capacity. Funct Ecol 26:216–226
Goldbogen JA, Hazen EL, Friedlaender AS, Calambokidis J, DeRuiter SL, Stimpert AK, Southall BL (2015) Prey density and distribution drive the three-dimensional foraging strategies of the largest filter feeder. Funct Ecol 29: 951–961
Goldbogen JA, Cade DE, Wisniewska DM, Potvin J and others (2019) Why whales are big but not bigger: physiological drivers and ecological limits in the age of ocean giants. Science 366:1367–1372
Hazen EL, Friedlaender AS, Goldbogen JA (2015) Blue whales (*Balaenoptera musculus*) optimize foraging efficiency by balancing oxygen use and energy gain as a function of prey density. Sci Adv 1:e1500469
Kotliar NB, Wiens JA (1990) Multiple scales of patchiness and patch structure: a hierarchical framework for the study of heterogeneity. Oikos 59:253–260
Lambert C, Authier M, Doray M, Dorémus G, Spitz J, Ridoux V (2019) Hide and seek in the Bay of Biscay—a functional investigation of marine megafauna and small pelagic fish interactions. ICES J Mar Sci 76:113–123
Levin SA (1992) The problem of pattern and scale in ecology: the Robert H. MacArthur award lecture. Ecology 73: 1943–1967
Lindeman RL (1942) The trophic-dynamic aspect of ecology. Ecology 23:399–417
MacArthur RH, Pianka ER (1966) On optimal use of a patchy environment. Am Nat 100:603–609
Mackas DL, Kieser R, Saunders M, Yelland DR, Brown RM, Moore DF (1997) Aggregation of euphausiids and Pacific hake (*Merluccius productus*) along the outer continental shelf off Vancouver Island. Can J Fish Aquat Sci 54: 2080–2096
Mannocci L, Boustany AM, Roberts JJ, Palacios DM and others (2017) Temporal resolutions in species distribution models of highly mobile marine animals: recommendations for ecologists and managers. Divers Distrib 23:1098–1109
Marra G, Wood SN (2011) Practical variable selection for generalized additive models. Comput Stat Data Anal 55: 2372–2387
Miller EJ, Potts JM, Cox MJ, Miller BS and others (2019) The characteristics of krill swarms in relation to aggregating Antarctic blue whales. Sci Rep 9:16487

Nichols RC, Cade DE, Kahane-Rapport S, Goldbogen J and others (2022) Intra-seasonal variation in feeding rates and diel foraging behaviour in a seasonally fasting mammal, the humpback whale. R Soc Open Sci 9:211674

NOAA (2016) Endangered and threatened species; identification of 14 distinct population segments of the humpback whale (*Megaptera novaeangliae*) and revision of species-wide listing. Fed Regist 81:62259

ODFW (Oregon Department of Fish and Wildlife) (2021) Draft conservation plan for reducing the impact of the Oregon ocean commercial Dungeness crab fishery on ESA-listed species off Oregon. Oregon Department of Fish and Wildlife Marine Resources Program, https://www.dfw.state.or.us/MRP/shellfish/commercial/crab/docs/2021/Public_CP_DRAFT_8.18.21.pdf

ODFW (2022) Oregon Dungeness crab fishery management plan. Oregon Department of Fish and Wildlife Marine Resources Program, https://www.dfw.state.or.us/MRP/shellfish/commercial/crab/docs/2022/Final_Dungeness_Crab_FMP_March_2022.pdf

Oldach E, Killeen H, Shukla P, Brauer E and others (2022) Managed and unmanaged whale mortality in the California Current Ecosystem. Mar Policy 140:105039

Orphanides CD, Jech JM, Palka DL, Collie J (2023) Relating marine mammal distribution to water column prey structure derived from echosounding. Mar Ecol Prog Ser 711: 101–119

Phillips EM, Chu D, Gauthier S, Parker-Stetter SL, Shelton AO, Thomas RE, Godo OR (2022) Spatiotemporal variability of euphausiids in the California Current Ecosystem: insights from a recently developed time series. ICES J Mar Sci 79:1312–1326

Piatt JF, Methven DA (1992) Threshold foraging behavior of baleen whales. Mar Ecol Prog Ser 84:205–210

R Core Team (2023) R: a language and environment for statistical computing. R Foundation for Statistical Computing, Vienna. www.r-project.org

Receveur A, Allain V, Menard F, Lebourges Dhaussy A and others (2022) Modelling marine predator habitat using the abundance of its pelagic prey in the tropical southwestern Pacific. Ecosystems 25:757–779

Rockwood RC, Elliott ML, Saenz B, Nur N, Jahncke J (2020) Modeling predator and prey hotspots: management implications of baleen whale co-occurrence with krill in Central California. PLOS ONE 15:e0235603

Ryan JP, Benoit-Bird KJ, Oestreich WK, Leary P and others (2022) Oceanic giants dance to atmospheric rhythms: ephemeral wind-driven resource tracking by blue whales. Ecol Lett 25:2435–2447

Santora JA, Mantua NJ, Schroeder ID, Field JC and others (2020) Habitat compression and ecosystem shifts as potential links between marine heatwave and record whale entanglements. Nat Commun 11:536

Stommel H (1963) Varieties of oceanographic experience: the ocean can be investigated as a hydrodynamical phenomenon as well as explored geographically. Science 139:572–576

Szesciorka AR, Demer DA, Santora JA, Forney KA, Moore JE (2023) Multiscale relationships between humpback whales and forage species hotspots within a large marine ecosystem. Ecol Appl 33:e2794

Torres LG (2017) A sense of scale: foraging cetaceans' use of scale-dependent multimodal sensory systems. Mar Mamm Sci 33:1170–1193

Torres LG, Read AJ, Halpin P (2008) Fine-scale habitat modeling of a top marine predator: Do prey data improve predictive capacity? Ecol Appl 18:1702–1717

Tyson RB, Friedlaender AS, Nowacek DP (2016) Does optimal foraging theory predict the foraging performance of a large air-breathing marine predator? Anim Behav 116: 223–235

Videsen SKA, Simon M, Christiansen F, Friedlaender A and others (2023) Cheap gulp foraging of a giga-predator enables efficient exploitation of sparse prey. Sci Adv 9: eade3889

Wiens JA (1989) Spatial scaling in ecology. Funct Ecol 3: 385–397

Wood SN (2011) Fast stable restricted maximum likelihood and marginal likelihood estimation of semiparametric generalized linear models. J R Stat Soc Series B Stat Methodol 73:3–36

Wood SN (2017) Generalized additive models: an introduction with R, 2nd edn. Chapman and Hall/CRC Press, Boca Raton, FL

Appendix

Table A1. Summary of rorqual whale–krill association models at each spatial scale (buffer radius). For each model, we report conditional and marginal deviance explained, the number of whale groups included (N_{wh}), and the absence, presence, and total number of data points in each model (N). For each smooth term (e.g. NASC 30–50 m, NASC 50–100 m, etc.), and the random effect (survey), we report estimated degrees of freedom (edf) and *F*-statistics. NASC (nautical area scattering coefficient; $m^2\ nmi^{-2}$) is a relative abundance metric for krill. All approximate significance of smooth terms showed $p < 0.0001$

Scale	Model	Buffer radius (km)	N_{wh}	N (absence, presence)	Conditional deviance explained (%)	Marginal deviance explained (%)	NASC 30–50 m	NASC 50–100 m	NASC 100–200 m	NASC 200–300 m	Survey
Very fine	A1	1	46	609261 (594477, 14784)	15.6	1.05	edf = 2.277, *F* = 232	edf =1.851, *F* = 343	edf = 3.909, *F* = 568.3	edf = 3.137, *F* = 277	edf =6.884, *F* = 1951
Very fine	A2	2	80	620041 (569424, 50617)	21.2	1.80	edf = 2.872, *F* = 5118	edf = 1.967, *F* = 7943	edf = 2.998, *F* = 5284	edf = 3.914, *F* = 5304	edf =6.903, *F* = 6972
Fine	A3	5	134	723978 (508332, 215646)	27.9	2.59	edf=3.923, *F* = 3414	edf = 2.975, *F* = 5323	edf = 3.612, *F* = 12799	edf = 3.541, *F* = 14544	edf =6.917, *F* = 18117
Meso	A4	20	178	1302550 (386409, 916141)	33.9	1.60	edf = 3.829, *F* = 1897	edf=3.944, *F* = 21315	edf = 2.997, *F* = 2462	edf = 2.985, *F* = 18754	edf =6.927, *F* = 47413

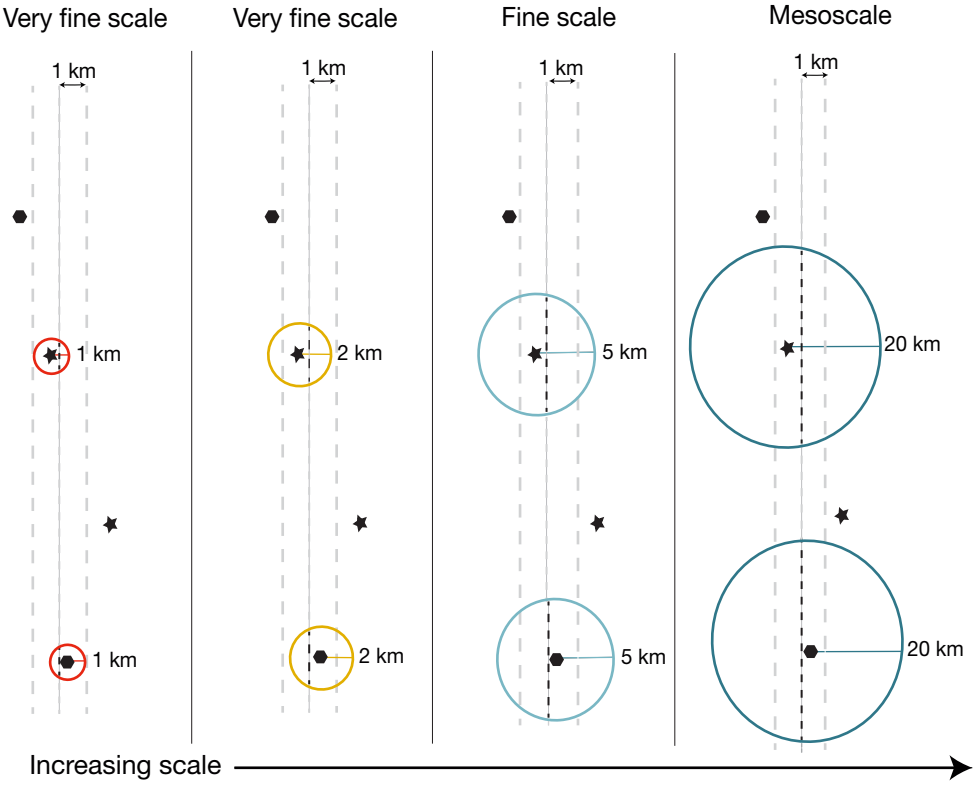

Fig. A1. Schematic representation of the inputs to the hierarchical scale and final models. The distance thresholds for included observations (coarse gray dashed lines) are illustrated around the ship's trackline (fine dashed line). Echosounder data along the trackline may be inside the buffers (black) or outside (gray), depending on model spatial scale. Buffer radii drawn at increasing spatial scales (circles color-coded from 1 to 20 km) are drawn around humpback whale observations (black stars) and fin or unidentified rorqual whale observations (black hexagons). The leftmost panel represents the data included in the 1 km 'very fine scale' model; model spatial scale increases moving right. The rightmost panel represents the inputs for the final, fine scale model. This schematic is not drawn to scale

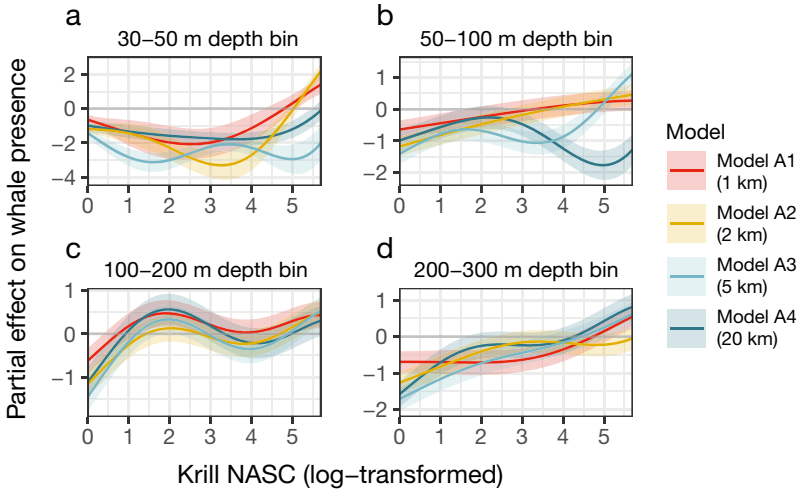

Fig. A2. All rorqual whale–krill relationships modeled across multiple depth bins and spatial scales. Response curves represent the effect of the smooth function upon the trend in rorqual whale presence, with higher values indicating higher predicted probability of occurrence. Shaded ribbons: 95% confidence intervals, colored per fitted trend. Log-transformed nautical area scattering coefficient (NASC, $m^2\,nmi^{-2}$; a relative abundance metric for krill) is shown on the *x*-axis, limited to the 5^{th}–95^{th} percentiles of its distribution. All variables have significant p-values ($p < 0.0001$)

Editorial responsibility: Peter Corkeron, Nathan, Queensland, Australia
Reviewed by: A. Friedlaender and 2 anonymous referees

Submitted: June 27, 2023
Accepted: December 12, 2023
Proofs received from author(s): February 5, 2024